Preprint typeset in JHEP style - HYPER VERSION

Constraining the Detailed Balance Condition in Hořava Gravity with Cosmic Accelerating Expansion

Chien-I Chiang[1,2♯], **Je-An Gu**[2†], **Pisin Chen**[1,2,3,4‡]

[1] *Department of Physics, National Taiwan University, Taipei 10617, Taiwan, R.O.C.,*
[2] *Leung Center for Cosmology and Particle Astrophysics, National Taiwan University, Taipei 10617, Taiwan, R.O.C.*
[3] *Graduate Institute of Astrophysics, National Taiwan University, Taipei 10617, Taiwan, R.O.C.*
[4] *Kavli Institute for Particle Astrophysics and Cosmology, SLAC National Accelerator Laboratory, Menlo Park, CA 94025, U.S.A.*

♯b95203016@ntu.edu.tw
†jagu@ntu.edu.tw
‡pisinchen@phys.ntu.edu.tw

Abstract: In 2009 Hořava proposed a power-counting renormalizable quantum gravity theory. Afterwards a term in the action that softly violates the detailed balance condition has been considered with the attempt of obtaining a more realistic theory in its IR-limit. This term is proportional to $\omega R^{(3)}$, where ω is a constant parameter and $R^{(3)}$ is the spatial Ricci scalar. In this paper we derive constraints on this IR-modified Hořava theory using the late-time cosmic accelerating expansion observations. We obtain a lower bound of $|\omega|$ that is nontrivial and depends on Λ_W, the cosmological constant of the three dimensional spatial action in the Hořava gravity. We find that to preserve the detailed balance condition, one needs to fine-tune Λ_W such that $-2.29 \times 10^{-4} < (c^2\Lambda_W)/(H_0^2\Omega_{\rm DE}) - 2 < 0$, where H_0 and $\Omega_{\rm DE}$ are the Hubble parameter and dark energy density fraction in the present epoch, respectively. On the other hand, if we do not insist on the detailed balance condition, then the valid region for Λ_W is much relaxed to $-0.39 < (c^2\Lambda_W)/(H_0^2\Omega_{\rm DE}) - 2 < 0.12$. We find that although the detailed balance condition cannot be ruled out, it is strongly disfavored.

Contents

1. Introduction

In 2009 Hořava proposed a power-counting renormalizable quantum gravity theory, which is non-relativistic in the high-energy, or UV, limit and recovers the Lorentz symmetry in the low-energy, or IR, limit [1, 2]. Various aspects of this theory have been widely pursued [3–30]. In addition to the theory itself, its various implications in cosmology have also drawn wide attention [31–34]. Specifically, there has been a large amount of effort in studying the cosmological perturbations [35–43], black hole properties [44–54], gravitational waves [55–59], dark energy phenomenology [60–63], observational constraints on the parameters of the theory [64, 65], and many others.

With regard to the background space-time expansion, Hořava gravity in principle modifies the GR Friedmann equation with additional terms stemming from its non-conventional gravity, thereby contributing to the dark sector. Accordingly, the current and future cosmic observations may provide significant constraints on Hořava gravity, especially when connecting it with the cosmic accelerating expansion.

In this context it was found that the effective Friedmann equation derived from Hořava gravity with the detailed balance condition would include a cosmological constant (CC) term and a radiation-like a^{-4} term [31, 32], where a is the scale factor in the Friedmann-Robertson-Walker (FRW) metric. This radiation-like term originates from the fourth-order spatial derivative terms in the Hořava action. On the other hand, if the detailed balance condition is violated, then there would be other dark terms induced.

Although the gravity action of the Hořava theory with the detailed balance condition recovers that of GR in the IR limit, its solution may not be so. For example, in [66] it was shown that the black hole solution does not recover the usual AdS-Schwarzschild black

hole solution in GR. In order to attain a more desirable IR behavior without abandoning the simplicity provided by the detailed balance condition in the UV limit, several authors introduced a soft violation of the detailed balance condition [1, 67, 68], namely, a term proportional to the spatial three-curvature $R^{(3)}$. In particular, an IR-modified Hořava theory that accommodates flat Minkowski vacuum was studied in [68]. The exact solutions of spherical symmetry with and without matter were obtained in [69].

A question then naturally arises: to what extent can the Hořava gravity violate the detailed balance condition? One possible means to address this question would be to derive constraints on the IR-modification terms and those obeying the detailed balance condition from cosmological observations. For this purpose we consider a cosmological model studied in [60] based on the IR-modified Hořava gravity, with the FRW metric describing the background space-time and with the energy content that includes radiation and dust matter.

In [60] Park showed that the Friedmann equation of this cosmological model contains additional a^{-4}, a^{-2}, and CC terms beyond that in GR. Park identified these terms as the effective dark energy (DE) that is responsible for the cosmic acceleration. The observations about the expansion history can in principle constrain the behavior of the (effective) dark energy and thereby constrain the Hořava gravity. To constrain this Hořava Effective Dark Energy (*HEDE*) by observations, an efficient approach is via a phenomenological parametrization of the relevant physical quantities that have been well studied. Once the relation between the model parameters and the phenomenological parameters is established, the constraints on the model can be obtained from those on the phenomenological parameters that have been derived from observations. Park considered the widely used Chevallier-Polarski-Linder (CPL) parameterization of the equation of state of dark energy [70, 71],

$$w_{\rm DE}(a) \equiv p_{\rm DE}/\rho_{\rm DE} = w_0 + w_a(1-a), \tag{1.1}$$

where the constraints on the phenomenological parameters w_0 and w_a from the updated observations have been well studied (see, for example, [72–76]).

Park [60] explored the feasibility of *HEDE* by considering three best-fit values of (w_0, w_a) obtained in [72, 73] where a non-flat universe was considered. It was suggested by Park that the existence of some *HEDE* models that satisfy these three best-fit values indicates the validity of *HEDE*. We note, however, that in principle the dark energy density of *HEDE* is determined once the values of (w_0, w_a) are given. As will be shown in the present paper, these three best-fit models predict the dark energy densities that are much smaller than that required by observations, and have thus already been ruled out.

In the present paper we pursue a more comprehensive test of the IR-modified Hořava theory and its resultant *HEDE* based on the current observations. We particularly emphasize that a complete test of *HEDE* based on the cosmic expansion must take into consideration not only the evolution of the dark energy density $\rho_{\rm DE}(a)$, which involves both the present value of $\Omega_{\rm DE}$ and the equation of state $w_{\rm DE}(a)$, but also the present value of the fractional density Ω_k of the spatial curvature.

Specifically, the present density fraction of dark energy $\Omega_{\rm DE}$ should be around 0.74 and that of the spatial curvature $\Omega_k < 0.01$ [75]. In addition, since in the dark sector the radiation-like term would be dominant in the early universe, its energy density must be smaller than the true radiation energy density Ω_r, otherwise *HEDE* would predict a later epoch of the matter-radiation equality and that in turn would be in conflict with the cosmic microwave background (CMB) and the big-bang nucleosynthesis (BBN) observational results. As will be shown in the present paper, the observational constraint on the dark energy equation of state $w_{\rm DE}$, together with the above three observational requirements, very tightly constrains *HEDE*. These observational constraints on *HEDE* favor the violation of detailed balance of Hořava gravity. We will present a lower bound on the extent of the violation.

This paper is organized as follows. In Sec. 2 we give a brief review of *HEDE*, a cosmological model based on the IR-modified Hořava theory. In Sec. 3 we discuss the general strategy that we utilize for the model test, which involves an approximate relation between the model parameters and the phenomenological parameters. In Sec. 4 we investigate the observational constraints on *HEDE* that are presented in the phenomenological parameter space. In Sec. 5 we show how the constraints on the phenomenological parameters are transcribed into that on the model parameters, and investigate its impact on the IR-modified Hořava gravity. In Sec. 6 we show the evolution patterns of the effective dark energy in the *HEDE* models that are consistent with observations. We conclude in Sec. 7.

2. Setup of the Model

To be self-contained, in this section we give a brief review of the IR-modified Hořava-gravity cosmological model that was investigated by Park [60]. The action of the IR-modified Hořava gravity reads

$$S_g = \int dtd^3x\sqrt{g}N\left[\frac{2}{\kappa^2}\left(K_{ij}K^{ij}-\lambda K^2\right)-\frac{\kappa^2}{2\nu^4}C_{ij}C^{ij}+\frac{\kappa^2\mu}{2\nu^2}\epsilon^{ijk}R^{(3)}_{il}\nabla_j R^{(3)l}{}_k\right. \tag{2.1}$$
$$\left.-\frac{\kappa^2\mu^2}{8}R^{(3)}_{ij}R^{(3)ij}+\frac{\kappa^2\mu^2}{8(3\lambda-1)}\left(\frac{4\lambda-1}{4}(R^{(3)})^2-\Lambda_W R^{(3)}+3\Lambda_W^2\right)+\frac{\kappa^2\mu^2\omega}{8(3\lambda-1)}R^{(3)}\right],$$

where the extrinsic curvature

$$K_{ij}=\frac{1}{2N}\left(\dot{g}_{ij}-\nabla_i N_j-\nabla_j N_i\right) \tag{2.2}$$

(the dot denotes the time derivative), the Cotton tensor

$$C^{ij}=\epsilon^{ik\ell}\nabla_k\left(R^{(3)j}{}_\ell-\frac{1}{4}R^{(3)}\delta^j_\ell\right), \tag{2.3}$$

and $\kappa, \lambda, \nu, \mu, \Lambda_W, \omega$ are constant parameters. Note that on the right-hand side of Eq.(2.1) the last term proportional to $\omega R^{(3)}$ induces the soft violation of the detailed balance condition. For a homogeneous and isotropic universe we consider a FRW metric of the form

$$ds^2=-c^2dt^2+a^2(t)\left[\frac{dr^2}{1-kr^2/R_0^2}+r^2\left(d\theta^2+\sin^2\theta d\phi^2\right)\right], \tag{2.4}$$

where $k = +1, 0, -1$ corresponds to a closed, a flat, and an open universe, respectively, and R_0 is the radius of spatial curvature of the universe in the present epoch. Assuming that the matter contribution is in the form of an ideal fluid with energy density ρ and pressure p, Park obtained [45]

$$\left(\frac{\dot{a}}{a}\right)^2 = \frac{\kappa^2}{6(3\lambda-1)}\left[\rho \pm \frac{3\kappa^2\mu^2}{8(3\lambda-1)}\left(\frac{-k^2}{R_0^4 a^4} + \frac{2k(\Lambda_W-\omega)}{R_0^2 a^2} - \Lambda_W^2\right)\right], \tag{2.5}$$

$$\frac{\ddot{a}}{a} = \frac{\kappa^2}{6(3\lambda-1)}\left[-\frac{1}{2}(\rho+3p) \pm \frac{3\kappa^2\mu^2}{8(3\lambda-1)}\left(\frac{k^2}{R_0^4 a^4} - \Lambda_W^2\right)\right], \tag{2.6}$$

where the analytic continuation $\mu^2 \to -\mu^2$ for Λ_W has been employed [45, 66, 77]. The upper (lower) sign corresponds to the case where $\Lambda_W < 0$ ($\Lambda_W > 0$).

Comparing them with the Einstein equations derived from GR with the FRW metric,

$$\left(\frac{\dot{a}}{a}\right)^2 = \frac{8\pi G}{3c^2}(\rho_{\rm m} + \rho_{\rm DE}) - \frac{c^2 k}{R_0^2 a^2}, \tag{2.7}$$

$$\frac{\ddot{a}}{a} = -\frac{4\pi G}{3c^2}\left[(\rho_{\rm m} + \rho_{\rm DE}) + 3(p_{\rm m} + p_{\rm DE})\right], \tag{2.8}$$

one can connect the Hořava parameters $\kappa, \lambda, \mu, \Lambda_W, \omega$ with the speed of light c, the Newton's constant G, and the effective dark energy density $\rho_{\rm DE}$ and pressure $p_{\rm DE}$, although the connection is not unique. Park defined the fundamental constants c and G as

$$c^2 = \frac{\kappa^4\mu^2|\Lambda_W|}{8(3\lambda-1)^2}, \; G = \frac{\kappa^2 c^2}{16\pi(3\lambda-1)}. \tag{2.9}$$

To ensure the positivity of the dark energy density as required by observations, we consider the case where $\Lambda_W > 0$ and identified the dark energy density and pressure as

$$\rho_{\rm DE} = \frac{3c^4}{16\pi G\Lambda_W}\left(\frac{H_0^4\Omega_k^2}{c^4 a^4} - \frac{2H_0^2\omega\Omega_k}{c^2 a^2} + \Lambda_W^2\right), \tag{2.10}$$

$$p_{\rm DE} = \frac{3c^4}{16\pi G\Lambda_W}\left(\frac{H_0^4\Omega_k^2}{3c^4 a^4} + \frac{2H_0^2\omega\Omega_k}{3c^2 a^2} - \Lambda_W^2\right), \tag{2.11}$$

where $\Omega_k = -(c^2 k)/(R_0^2 H_0^2)$. The equation of state parameter is then

$$w_{\rm DE} \equiv \frac{p_{\rm DE}}{\rho_{\rm DE}} = \frac{H_0^4\Omega_k^2 + 2c^2 H_0^2\omega\Omega_k a^2 - 3c^4\Lambda_W^2 a^4}{3H_0^4\Omega_k^2 - 6c^2 H_0^2\omega\Omega_k a^2 + 3c^4\Lambda_W^2 a^4}. \tag{2.12}$$

From Eq. (2.10) we obtain

$$\frac{\rho_{\rm DE}}{\rho_c} = \left(\frac{H_0^2\Omega_k^2}{2c^2\Lambda_W}\right)\frac{1}{a^4} - \left(\frac{\Omega_k\omega}{\Lambda_W}\right)\frac{1}{a^2} + \frac{c^2}{2H_0^2}\Lambda_W \tag{2.13}$$

$$\equiv \Omega_1 a^{-4} + \Omega_2 a^{-2} + \Omega_3, \tag{2.14}$$

where the critical energy density $\rho_c = (3H_0^2 c^2)/(8\pi G)$ and

$$\Omega_1 = \frac{H_0^2\Omega_k^2}{2c^2\Lambda_W} \geq 0, \quad \Omega_2 = -\frac{\Omega_k\omega}{\Lambda_W}, \quad \Omega_3 = \frac{c^2\Lambda_W}{2H_0^2} > 0. \tag{2.15}$$

As shown by the above formulae, this effective dark energy consists of three components that are radiation-like, curvature-like and CC-like, respectively. It involves three model parameters: $\{\Omega_k, \omega, \Lambda_W\}$. The first parameter stems from the FRW metric ansatz, and the last two from the Hořava gravity action. Note that for a flat universe this effective dark energy behaves as a CC and accordingly this model is the same as the CC dark energy model in GR, i.e. flat ΛCDM, which is consistent with all the current observational results. In the present paper we will consider a nonzero Ω_k for possible deviation from ΛCDM.

3. Model Parameters and Phenomenological Parameters

To compare the Hořava Effective Dark Energy (*HEDE*) model with observational results, one effective approach is to employ a phenomenological parametrization of the relevant quantities, whose observational constraints have been well studied, as a mediator to facilitate the comparison. The observational constraints on the model can be obtained from those on the phenomenologically parametrized quantities by invoking an approximate relation between the model parameters and the phenomenological parameters.

In *HEDE* the model parameters include $\{\Omega_k, \omega, \Lambda_W\}$, which determine the dark energy behavior. That is, the dark energy density $\rho_{\rm DE}(a)$, as well as $w_{\rm DE}(a)$, is a function of $\{\Omega_k, \omega, \Lambda_W\}$. Phenomenologically, the evolution of dark energy is determined by the present density fraction $\Omega_{\rm DE}$ and its equation of state parameter $w_{\rm DE}$. Here we invoke the widely used CPL parameterization [70, 71] of $w_{\rm DE}$ in Eq. (1.1): $w_{\rm DE} = w_0 + w_a(1-a)$. In addition, since the spatial curvature Ω_k is involved in the model parameters, it should also be included in the phenomenological parameter space when connecting to the model space. In summary, the phenomenological parameters are $\{\Omega_k, \Omega_{\rm DE}, w_0, w_a\}$. Accordingly, we have a three-dimensional model parameter space and a four-dimensional phenomenological parameter space. A mapping between them is required for constraining the model via the observational constraints on the phenomenological parameters.

The relation between $\Omega_{\rm DE}$ and $\{\Omega_k, \omega, \Lambda_W\}$ can be obtained from Eq. (2.13) by setting $a = 1$:

$$\Omega_{\rm DE}(\Omega_k, \omega, \Lambda_W) = \frac{H_0^2\Omega_k^2}{2c^2\Lambda_W} - \frac{\Omega_k\omega}{\Lambda_W} + \frac{c^2}{2H_0^2}\Lambda_W. \tag{3.1}$$

Following Park [60], we connect the model parameters $\{\omega, \Lambda_W\}$ with the phenomenological parameters by firstly expanding $w_{\rm DE}$ in (2.12) around $a = 1$ as

$$w_{\rm DE} = w_{\rm DE}|_{a=1} - w'_{\rm DE}\big|_{a=1}(1-a) + \cdots, \tag{3.2}$$

where the prime denotes the derivative with respect to a, and then identify $w_{\rm DE}|_{a=1}$ and $-w'_{\rm DE}|_{a=1}$ as w_0 and w_a in the CPL parameterization. As a result, the approximate relation between $\{\omega, \Lambda_W\}$ and $\{w_0, w_a\}$ reads

$$w_0(\Omega_k, \omega, \Lambda_W) = \frac{H_0^4\Omega_k^2 + 2c^2H_0^2\omega\Omega_k - 3c^4\Lambda_W^2}{3H_0^4\Omega_k^2 - 6c^2H_0^2\omega\Omega_k + 3c^4\Lambda_W^2}, \tag{3.3}$$

$$w_a(\Omega_k, \omega, \Lambda_W) = -\frac{8c^2H_0^2\Omega_k\left(H_0^4\omega\Omega_k^2 - 2c^2H_0^2\Omega_k\Lambda_W^2 + c^4\omega\Lambda_W^2\right)}{3\left(H_0^4\Omega_k^2 - 2c^2H_0^2\omega\Omega_k + c^4\Lambda_W^2\right)^2}, \tag{3.4}$$

or equivalently,

$$\omega = -\frac{(1-2w_0-3w_0^2-w_a)H_0^2\Omega_k}{(1+4w_0+3w_0^2+w_a)c^2}, \tag{3.5}$$

$$\Lambda_W^2 = \frac{(-1+9w_0^2+3w_a)H_0^4\Omega_k^2}{3(1+4w_0+3w_0^2+w_a)c^4}. \tag{3.6}$$

The required mapping between $\{\Omega_k, \omega, \Lambda_W\}$ and $\{\Omega_k, \Omega_{\rm DE}, w_0, w_a\}$ is given by Eqs. (3.1), (3.3) and (3.4). It maps the 3D model space to a 3D hypersurface in the 4D phenomenological parameter space.

Regarding the observational constraints, as stated in Sec. 1, we assume $\Omega_{\rm DE} \approx 0.74$, $\Omega_k < 0.01$ [75], $\Omega_1 < \Omega_r$, and the constraint on $w_{\rm DE}$ obtained in [74]. For simplicity, we fix $\Omega_{\rm DE} = 0.74$. This reduces the dimension of the phenomenological parameter space from four to three: $\{\Omega_k, w_0, w_a\}$, and that of the model space from three to two, i.e. a 2-dimensional surface in the 3D space $\{\Omega_k, \omega, \Lambda_W\}$. This 2D surface corresponds to the relation $\Omega_k = \Omega_k(\omega, \Lambda_W)$ obtained from Eq. (2.13) with $\rho_{\rm DE}(a=1)/\rho_c = 0.74$. In this case the relations in Eqs. (3.1), (3.3) and (3.4) become $\Omega_{\rm DE} = \Omega_{\rm DE}(\omega, \Lambda_W)$, $w_0 = w_0(\omega, \Lambda_W)$ and $w_a = w_a(\omega, \Lambda_W)$. They map the reduced 2D model space $\{\Omega_k(\omega, \Lambda_W), \omega, \Lambda_W\}$ to a 2D surface $\{\Omega_k(\omega, \Lambda_W), w_0(\omega, \Lambda_W), w_a(\omega, \Lambda_W)\}$ in the reduced 3D phenomenological parameter space $\{\Omega_k, w_0, w_a\}$. Then, the observational constraint on the model is represented by the intersection of this 2D surface and the well-studied, observationally allowed regions of the 3D phenomenological parameter space. We note that the spatial curvature is well constrained. The upper bound of $|\Omega_k|$ is around 0.01 and could be even smaller [75]. Thus, the allowed region in the 3D phenomenological parameter space is very thin in the Ω_k direction. Accordingly, as a good approximation after imposing the constraint $\Omega_k < 0.01$, we will simply consider the constraints on the $\{w_0, w_a\}$ plane when taking the above-mentioned intersection that presents the valid region of the model.

4. Constraints on the Phenomenological Parameter Space

x As commented in [60], for the sake of self-consistency one should require $\Lambda_W^2 \geq 0$. From Eq. (3.6), this in turn requires that

$$\begin{aligned} &\left\{w_a > -1-4w_0-3w_0^2,\ w_a \geq (1-9w_0^2)/3\right\} \\ \text{or}\ &\left\{w_a < -1-4w_0-3w_0^2,\ w_a \leq (1-9w_0^2)/3\right\}. \end{aligned} \tag{4.1}$$

To simplify the following calculations, we define

$$A = 1+4w_0+3w_0^2+w_a, \tag{4.2}$$

$$B = -1+9w_0^2+3w_a. \tag{4.3}$$

The self-consistency condition in Eq. (4.1) then reads

$$\{A>0, B\geq 0\} \quad \text{or} \quad \{A<0, B\leq 0\}. \tag{4.4}$$

The valid region on the $\{w_0, w_a\}$ plane for this self-consistency condition is presented in Figure 1 by the shaded area.

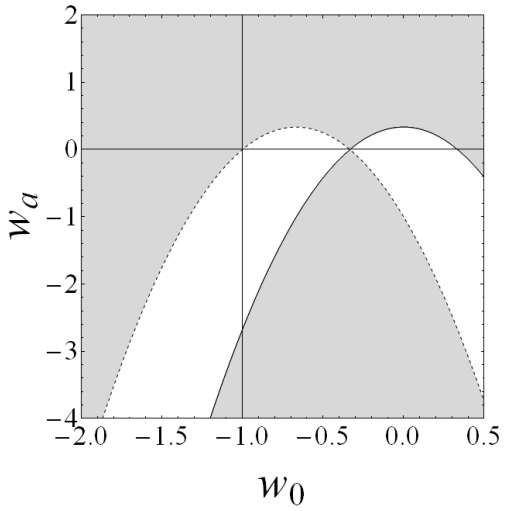

Figure 1: The valid (shaded) region for the self-consistency condition $\Lambda_W^2 > 0$.

Rewriting Eqs. (3.5) and (3.6) in terms of A and B, we have

$$\omega = \frac{3A + B - 8}{6A}\left(\frac{H_0^2\Omega_k}{c^2}\right), \ \Lambda_W = \sqrt{\frac{B}{3A}}\left(\frac{H_0^2}{c^2}\right)|\Omega_k|. \tag{4.5}$$

Substituting Eq. (4.5) into Eq. (3.1), we obtain

$$|\Omega_k| = \mathrm{sgn}(A)\frac{\sqrt{3}}{4}\sqrt{AB}\ \Omega_{\mathrm{DE}}, \tag{4.6}$$

where $\mathrm{sgn}(A)$ denotes the sign of A. For a positive dark energy density, this relation requires $A \geq 0$, which, as combined with Eq. (4.4), leads to

$$\{A > 0, B \geq 0\}, \tag{4.7}$$

thereby excluding the bottom middle shaded area in Figure 1.

The current observations suggest $\Omega_{\mathrm{DE}} \approx 0.74$ and $|\Omega_k| < 0.01$ [75]. With Eqs. (4.6) and (4.7), these two requirements give a stringent constraint on the parameters A and B (i.e. w_0 and w_a):

$$0 < AB < \left(\frac{4}{\sqrt{3}}\frac{0.01}{0.74}\right)^2 \cong 9.74 \times 10^{-4}. \tag{4.8}$$

This constraint largely shrinks the allowed region in the parameter space, which is presented by the shaded region in Figure 2.

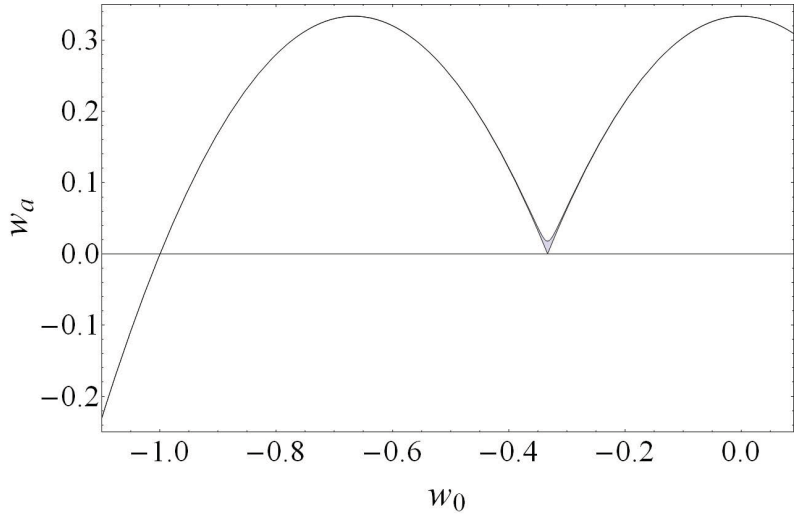

Figure 2: The shaded area shows the largely reduced allowed region for the observational requirements, $\Omega_{\rm DE} \approx 0.74$ and $|\Omega_k| < 0.01$, that lead to the constraint in Eq. (4.8).

As indicated in Eq. (2.14), the effective dark energy sector of the (IR-modified) *HEDE* model consists of a radiation-like (Ω_1), a curvature-like (Ω_2), and a constant (Ω_3) term. In the early universe when a is small, the radiation-like term dominates the effective dark energy sector. Such a term, if too large, would cause the epoch of the matter-radiation equality happened at a time that is later than that suggested by the observational results about CMB and BBN. Specifically, this term may contribute to the effective relativistic degrees of freedom in the early universe. In the CMB analysis the radiation is usually subdivided into two categories: (i) photons and (ii) effective neutrinos (including neutrinos and other effective relativistic particles). Accordingly,

$$\Omega_r = \Omega_\gamma + \Omega_\nu = \Omega_\gamma(1 + 0.2271 N_{eff}), \tag{4.9}$$

where Ω_r is the present radiation energy density fraction, and N_{eff} is the number of effective neutrino species. The WMAP results suggest that $\Omega_r \cong 8.47 \times 10^{-5}$ and $N_{eff} \approx 4$ [75]. Accordingly the effective neutrinos have a comparable contribution to the radiation energy density. Regarding the radiation-like term from Hořava gravity as a source of the effective neutrinos, we obtain an upper bound of Ω_1 given by $0.2271 N_{eff}\Omega_\gamma$, which is of the same order as Ω_r. This leads us to impose the constraint,

$$\Omega_1 < \Omega_r \cong 8.47 \times 10^{-5}. \tag{4.10}$$

Substituting Eqs. (4.5) and (4.6) into the definition of Ω_1 in Eq. (2.15), we obtain $\Omega_1 = 3|A|\Omega_{\rm DE}/8$, from which and Eq. (4.7) the above constraint requires

$$0 < A < \frac{8\Omega_r}{3\Omega_{\rm DE}} \approx 3.05 \times 10^{-4}. \tag{4.11}$$

This tightly constrained region is presented in Figure 3 by the black area which is so narrow that it looks like a black curve. In this figure we also show the constraint given in Eq. (4.8),

which is presented by the gray area. For $w_0 < -1/3$, it largely overlaps with the black narrow region.

In addition, in Figure 3 we show the 1σ (long-dashed contour) and the 2σ (dot-dashed contour) observational constraints of w_0 and w_a obtained in [74] from the combined data set that includes the SN-Ia data from the Constitution Set, the CMB measurement from the five-year WMAP, and the BAO measurement from SDSS and 2dFGRS. The intersection of all the above-mentioned allowed regions gives the valid IR-modified Hořava Effective Dark Energy model, which is the black narrow region enclosed by the long-dashed (1σ) or the dot-dashed (2σ) contour.

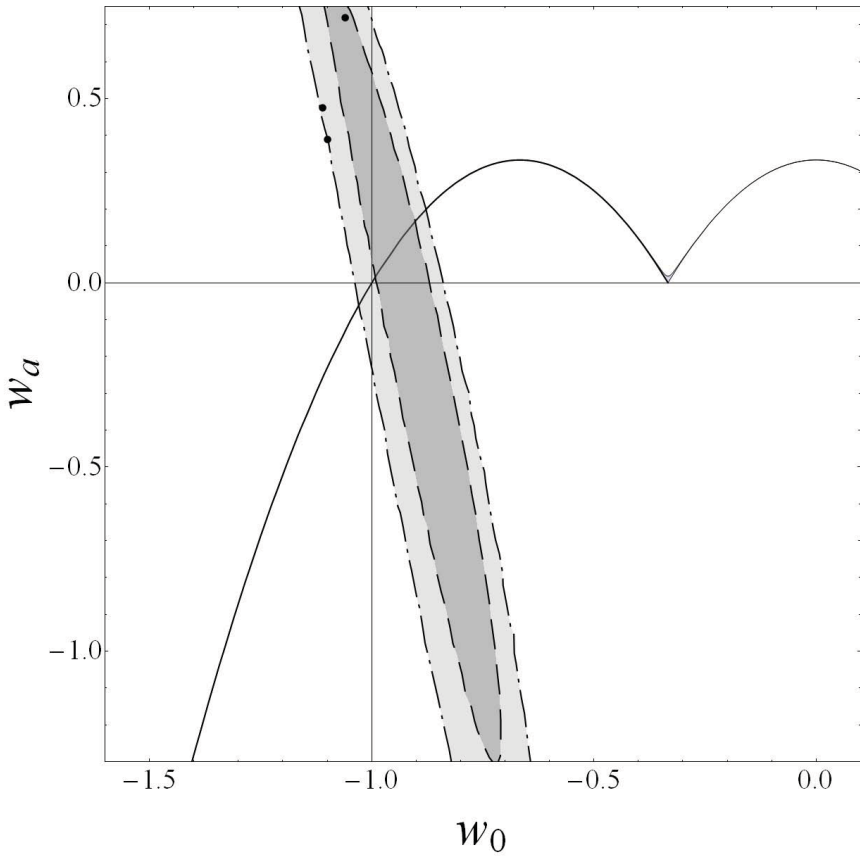

Figure 3: Various constraints on the w_0-w_a plane for the IR-modified Hořava Effective Dark Energy (*HEDE*) model. The constraints are given in Eqs. (4.8) and (4.11), and in [74]. The long-dashed and the dot-dashed contour respectively present the 1σ and the 2σ constraint on $\{w_0, w_a\}$, which is obtained in [74] from the current SN Ia, CMB and BAO data. The narrow gray region presents the constraint in Eq. (4.8) for the requirement $|\Omega_k| < 0.01$. The narrow black region that nearly overlaps with the narrow gray region for $w_0 < -1/3$ presents the constraint in Eq. (4.11) for the requirement $\Omega_1 < \Omega_r$. The intersection of these three kinds of allowed regions gives the valid *HEDE* model. The three black dots denote the best-fit models Park considered in [60], none of which is in the valid region.

5. Constraining the IR-modified Hořava Gravity

To constrain the IR-modified Hořava gravity, here we transfer the observational constraints on the phenomenological parameters to the *HEDE* model via the mapping between the phenomenological parameter space and the model space. This mapping is given in Eqs. (3.5) and (3.6), i.e., in Eq. (4.5), where $|\Omega_k|$ is a function of A and B, as given in Eq. (4.6), after we fix $\Omega_{\rm DE} = 0.74$. With Eqs. (4.6) and (4.7) substituted into Eq. (4.5), this mapping can be rewritten as

$$\tilde{\omega} = s_k \frac{\sqrt{3}}{24}(3A + B - 8)\sqrt{\frac{B}{A}}, \tag{5.1}$$

$$\tilde{\Lambda}_W = \frac{1}{4}B, \tag{5.2}$$

where the two dimensionless parameters $\tilde{\omega}$ and $\tilde{\Lambda}_W$ are defined as

$$\tilde{\omega} = \frac{c^2\omega}{H_0^2\Omega_{\rm DE}}, \quad \tilde{\Lambda}_W = \frac{c^2\Lambda_W}{H_0^2\Omega_{\rm DE}}, \tag{5.3}$$

and s_k denotes the sign of Ω_k.

In the valid region, i.e. the black narrow region enclosed by the 2σ contour in Figure 3, we have the constraints $0 < A < 3.05\times10^{-4}$, as required in Eq. (4.10), and $6.44 < B < 8.48$. From the above mapping and the constraints on A and B, we obtain

$$\tilde{\omega}\left(\epsilon, \tilde{\Lambda}_W\right) = \frac{s_k}{2}\left[\left(\tilde{\Lambda}_W - 2\right) + \epsilon\right]\sqrt{\frac{\tilde{\Lambda}_W}{\epsilon}}, \tag{5.4}$$

where

$$0 < \epsilon \equiv \frac{3}{4}A < 2.29 \times 10^{-4}, \tag{5.5}$$

$$-0.39 < \tilde{\Lambda}_W - 2 < 0.12. \tag{5.6}$$

For more details, the constraint on $\{\tilde{\omega}, \tilde{\Lambda}_W\}$ can be read as follows.

$$\begin{aligned}
-\infty < s_k\tilde{\omega} < s_k\tilde{\omega}(\epsilon_{max}) < 0 \quad &\text{as} \quad \tilde{\Lambda}_W \le 2 - \epsilon_{max}\,, \\
-\infty < s_k\tilde{\omega} < s_k\tilde{\omega}(\epsilon_{max}) > 0 \quad &\text{as} \quad 2 - \epsilon_{max} < \tilde{\Lambda}_W < 2\,, \\
0 < s_k\tilde{\omega} < \sqrt{\epsilon_{max}/2} \quad &\text{as} \quad \tilde{\Lambda}_W = 2\,, \\
\sqrt{\tilde{\Lambda}_W(\tilde{\Lambda}_W - 2)} < s_k\tilde{\omega} < \infty \quad &\text{as} \quad 2 < \tilde{\Lambda}_W \le 2 + \epsilon_{max}\,, \\
0 < s_k\tilde{\omega}(\epsilon_{max}) < s_k\tilde{\omega} < \infty \quad &\text{as} \quad \tilde{\Lambda}_W > 2 + \epsilon_{max}\,,
\end{aligned} \tag{5.7}$$

where $\epsilon_{max} = 2.29 \times 10^{-4}$. This constraint is presented in Figure 4, where the dark region and the light region correspond to $s_k = +$ and $s_k = -$, i.e. $\Omega_k > 0$ and $\Omega_k < 0$, respectively.

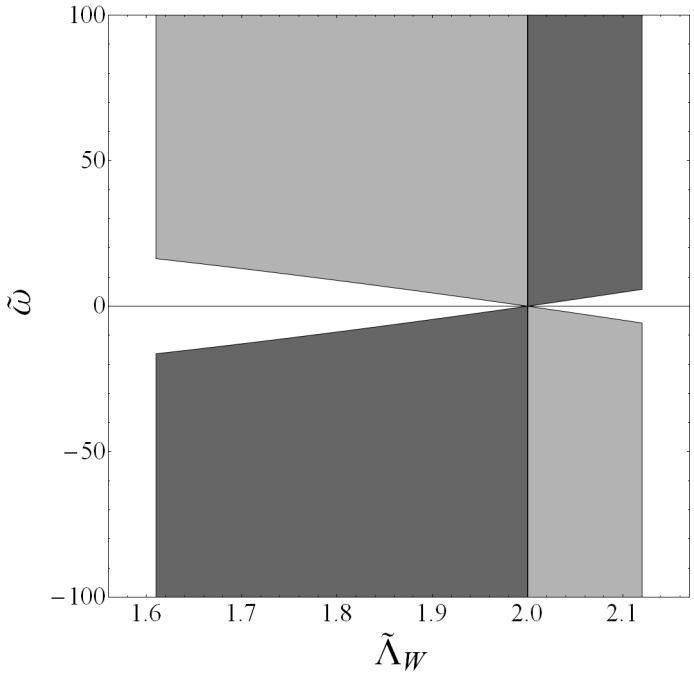

Figure 4: The valid $\tilde{\omega}$-$\tilde{\Lambda}_W$ region corresponding to the valid region in the w_0-w_a space. The dark and the light region correspond to $\Omega_k > 0$ and $\Omega_k < 0$, respectively.

As shown in Figure 4, $\tilde{\Lambda}_W$ is restricted to values between 1.61 and 2.12, and $|\tilde{\omega}|$ has a nontrivially lower limit but no upper limit. We note that for $\tilde{\omega} = 0$ the allowed region is almost a point, specifically,

$$-2.29 \times 10^{-4} < \tilde{\Lambda}_W - 2 < 0. \tag{5.8}$$

That is, in the case where detailed balance is preserved ($\omega = 0$) we need to fine-tune the value of Λ for the *HEDE* model to be consistent with observational results. Thus, the cosmological test strongly disfavors, although does not rule, the Hořava action that preserves detailed balance. On the contrary, for large $|\tilde{\omega}|$ the full range of $\tilde{\Lambda}_W$, $(1.61, 2.12)$, is allowed. Moreover, there is no upper limit to $|\tilde{\omega}|$. Accordingly, the observational results suggest the breaking of the detailed balance condition.

Note that the curvature-like effective energy term in Eq. (2.14), as originated from the soft violation of detailed balance, remains finite when $\tilde{\omega}$ goes to infinity. This can be seen in the following.

$$\Omega_2 = -\frac{\Omega_k \omega}{\Lambda_W} = \frac{\Omega_{\rm DE}}{8}(8 - 3A - B), \tag{5.9}$$

where $\Omega_{\rm DE} \approx 0.74$, $0 < A < 3.05 \times 10^{-4}$ and $6.44 < B < 8.48$ for the valid region. We emphasize that even though at the action level the magnitude of the soft violation can be arbitrarily large with no upper limit, the corresponding effective energy may still be tightly constrained.

6. Possible Behavior of the Effective Dark Energy

Recall Eqs. (2.13) and (2.14), the *HEDE* consists of the radiation-like ($\Omega_1 a^{-4}$), the curvature-like ($\Omega_2 a^{-2}$) and the constant-like (Ω_3) sectors:

$$\frac{\rho_{\rm DE}}{\rho_c} = \left(\frac{H_0^2\Omega_k^2}{2c^2\Lambda_W}\right)\frac{1}{a^4} - \left(\frac{\Omega_k\omega}{\Lambda_W}\right)\frac{1}{a^2} + \frac{c^2}{2H_0^2}\Lambda_W \tag{6.1}$$

$$\equiv \Omega_1 a^{-4} + \Omega_2 a^{-2} + \Omega_3. \tag{6.2}$$

Substituting Eqs. (3.5), (3.6) and (4.6) into Eq. (2.15), we obtain

$$\Omega_1 = \frac{3\Omega_{\rm DE}}{8}(1 + 4w_0 + 3w_0^2 + w_a), \tag{6.3}$$

$$\Omega_2 = \frac{-3\Omega_{\rm DE}}{4}(-1 + 2w_0 + 3w_0^2 + w_a), \tag{6.4}$$

$$\Omega_3 = \frac{\Omega_{\rm DE}}{8}(-1 + 9w_0^2 + 3w_a). \tag{6.5}$$

Note that $\Omega_1+\Omega_2+\Omega_3 = \Omega_{\rm DE}$ as required. The requirement $\Omega_{\rm DE} = 0.74$ and the constraint on $\{w_0, w_a\}$ give an allowed region in the $\{\Omega_1, \Omega_2, \Omega_3\}$ space: a plane $\Omega_1 + \Omega_2 + \Omega_3 = 0.74$ bounded by the box $\{0 < \Omega_1 < 8 \times 10^{-6}, -0.05 < \Omega_2 < 0.15, 0.59 < \Omega_3 < 0.78\}$ corresponding to the 2σ contour on $\{w_0, w_a\}$.

To show the possible evolution patterns of the *HEDE*, we consider three sample cases, **DE.1**, **DE.2** and **DE.3**, corresponding to three points in the narrow valid region in Figure 3. The values of $\{w_0, w_a; \Omega_1, \Omega_2, \Omega_3\}$ in these three cases are as follows.

	w_0	w_a	Ω_1	Ω_2	Ω_3
DE.1	-1.00	1.14×10^{-4}	3.18×10^{-5}	-6.35×10^{-5}	0.740
DE.2	-0.95	9.27×10^{-2}	4.24×10^{-5}	5.54×10^{-2}	0.685
DE.3	-0.90	1.70×10^{-1}	3.18×10^{-6}	1.11×10^{-1}	0.629

(6.6)

The evolution of the energy density in these three cases is shown in Figure 5. These three cases have the same density fraction at present, $\Omega_{\rm DE} = 0.74$, and share similar evolution patterns in the late times up to $\ln(1+z) \approx 0.25$. **DE.1** resembles ΛCDM at low redshifts. Its energy density remains nearly constant for $\ln(1+z) < 2.0$. This is because Ω_1 and Ω_2 are both extremely small in this case. In the cases of **DE.2** and **DE.3** the energy densities increase with z rapidly for $\ln(1+z) > 0.25$ due to the Ω_2 term. Generally speaking, it is the difference in Ω_2 that makes the evolution patterns distinct from each other in the interval $0.25 < \ln(1+z) < 3.5$. In the early universe, the radiation-like term in *HEDE* would dominate. Hence for $\ln(1+z) > 5$ the slopes of $\ln(\rho/\rho_c)$ versus $\ln(1+z)$ in different cases are roughly the same. The value of Ω_1 determines the value of $\ln(\rho/\rho_c)$ at high redshifts. The cases with larger Ω_1 have larger energy densities in the early times. Nevertheless, in the early times the energy density of *HEDE* should be smaller than that of radiation, as required in Eq. (4.10).

In Figure 6 we show the redshift dependence of the ratio ρ_i/ρ_t, where ρ_i stands for the energy density of **DE.1**, **DE.2**, **DE.3**, matter or radiation, and ρ_t for the total energy

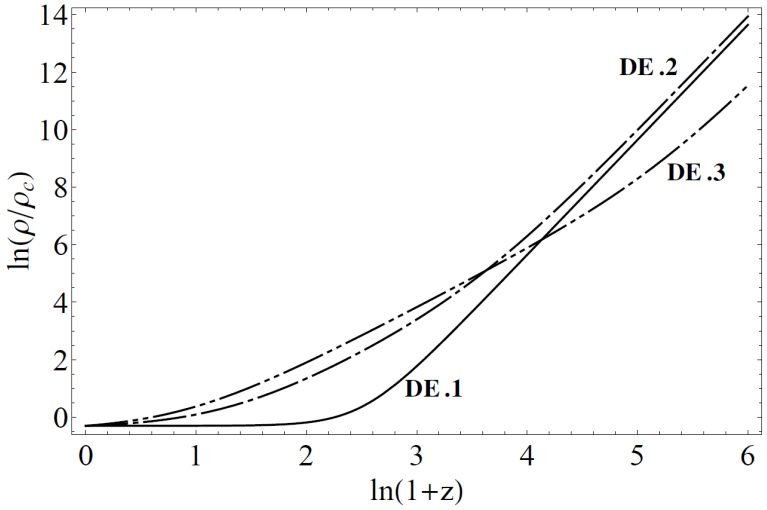

Figure 5: The energy density evolution patterns in three sample cases. The solid, the dot-dashed and the double-dot-dashed line correspond to **DE.1**, **DE.2** and **DE.3**, respectively.

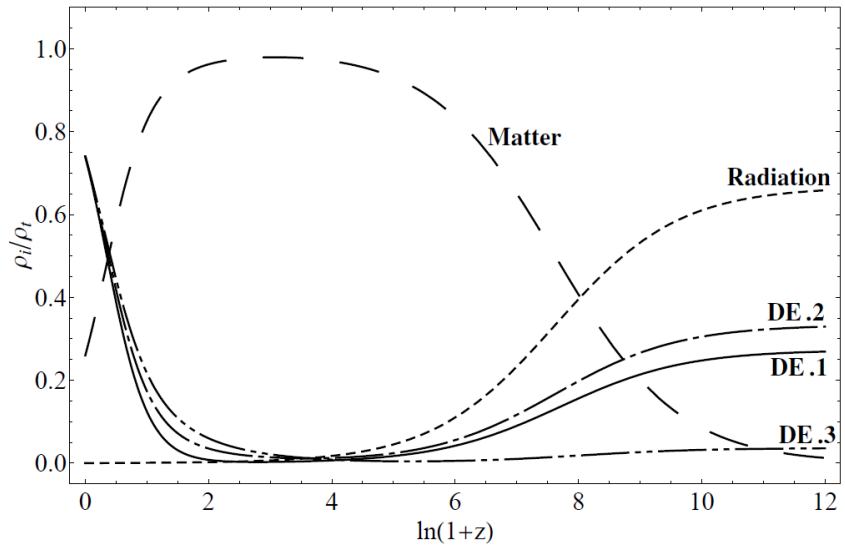

Figure 6: The redshift dependence of the contribution of different energy contents to the total energy density. The solid, dot-dashed, double-dot-dashed, long-dashed, and short-dashed lines correspond to **DE.1**, **DE.2**, **DE.3**, matter and radiation, respectively.

density. The evolution of the three cases nearly coincide with each other after the time when $\ln(1+z) \approx 0.5$ (i.e. $z \approx 0.65$), around which the crossing between the *HEDE* and the matter energy density at low redshift happens. This is because after the crossing the constant-like (Ω_3) term dominates the dark sector, while these three cases have similar Ω_3. Before this crossing, the three cases behave differently. For $\ln(1+z) < 4$ the contribution of the *HEDE* to the total energy decreases with z, and the decreasing is more rapid in **DE.1** than in **DE.2** and **DE.3**. The main reason is that Ω_2 in **DE.1** is negative. In general, $\rho_{\rm DE}/\rho_t$ decreases with z more rapidly for smaller Ω_2. For $\ln(1+z) > 4$ (i.e., for $z > 50$), the

contribution of the *HEDE* to the total energy increases with z. This is a reflection of the dominance of the radiation-like (Ω_1) term over the other two terms in the dark sector. The slop of this increment and the contribution of the *HEDE* at high redshifts are determined by the value of Ω_1. In the case with larger Ω_1, $\rho_{\rm DE}$ increases with z more rapidly and $\rho_{\rm DE}/\rho_t$ is larger for $\ln(1+z) > 4$. However, the contribution of the *HEDE* would be smaller than that of radiation in the early times, as required in Eq. (4.10).

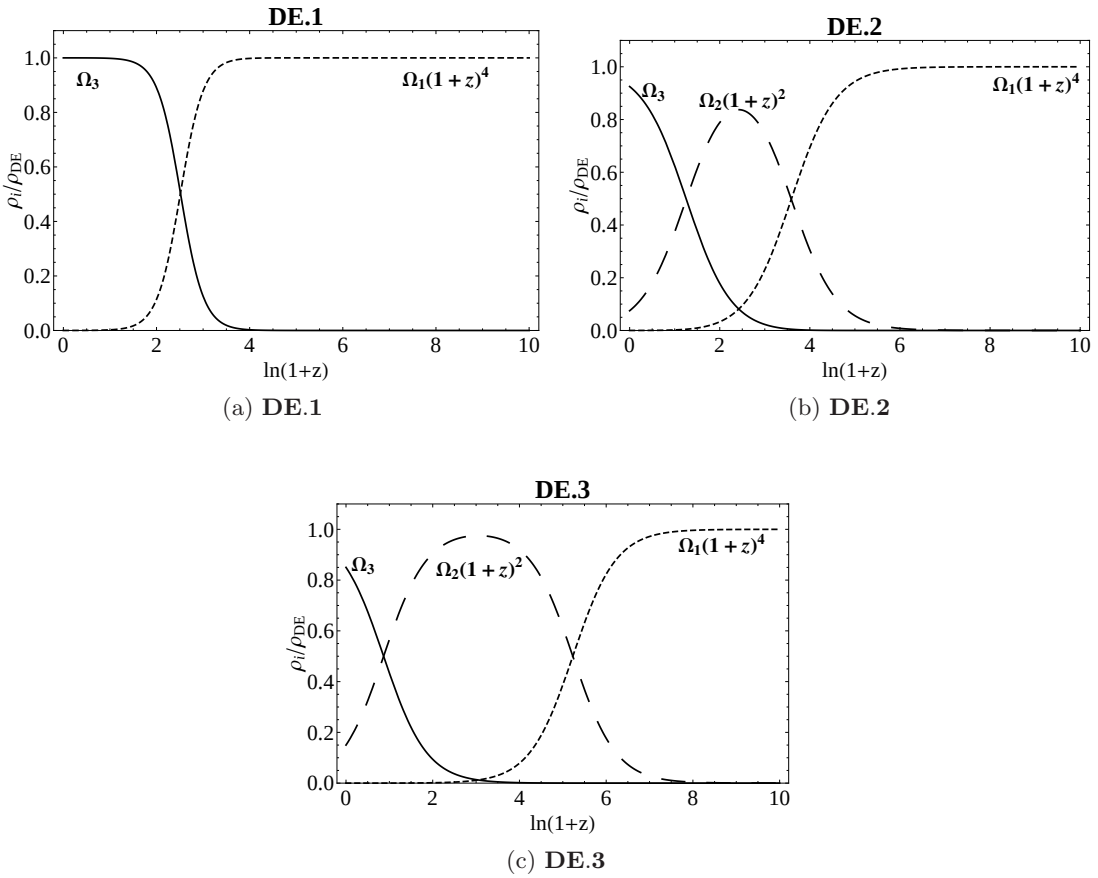

(a) **DE.1** (b) **DE.2**

(c) **DE.3**

Figure 7: The redshift dependence of the contribution of the three dark terms in the *HEDE* energy density for the three cases, **DE.1**, **DE.2** and **DE.3**. The solid, the long-dashed, and the short-dashed line correspond to the constant-like, the curvature-like, and the radiation-like term, respectively.

In Figure 7 we show the redshift dependence of the contribution of the three terms, $\{\Omega_1(1+z)^4, \Omega_2(1+z)^2, \Omega_3\}$, in the *HEDE* energy density for the three cases in Eq. (6.6). For all the three cases, the constant-like (Ω_3) term dominates the dark sector in the late times, while the radiation-like (Ω_1) term dominates in the early times. Whether there exists a period of the dominance of the curvature-like (Ω_2) term depends on the magnitude of Ω_2. For **DE.1**, the contribution of the term $\Omega_2(1+z)^2$ is much smaller than the other two terms. Hence in Figure 7a the line corresponding to this term cannot be seen. For the **DE.2** and **DE.3** cases, the curvature-like term dominates the dark sector during a "middle age". The precise period of such "middle age" varies from case to case. In general,

for larger Ω_2, the dominance of the curvature-like term starts earlier and ends later, with larger contribution from this term to the *HEDE*.

7. Summary and Discussion

In this paper we test the IR-modified Hořava gravity from the cosmological point of view, in particular, from the viewpoint of cosmic expansion. We conclude that the Hořava gravity with soft violation of the detailed balance condition is consistent with the current observational results on the expansion history of the universe. Specifically, this gravity theory can generate the late-time cosmic acceleration with the behavior that is well consistent with observations. We note that the Hořava gravity with the detailed balance condition, though not ruled out, requires fine-tuning Λ_W such that $-2.29\times10^{-4} < (c^2\Lambda_W)/(H_0^2\Omega_{\rm DE}) - 2 < 0$ in order to fit the observational data. This result, together with previous studies [66, 78], suggests that the breaking of the detailed balance condition, at least softly, is necessary to render Hořava gravity a more realistic IR-limit.

We obtained the observational constraints on two model parameters, Λ_W and ω, i.e., the cosmological constant of the three dimensional Einstein-Hilbert action and the coefficient of the soft violation term. The parameter Λ_W is well-constrained and it should be of the order of the inverse square of the Hubble length, H_0^2/c^2. More precisely, we found that Λ_W, in units of (H_0^2/c^2), is bounded within a small range, $(1.61\Omega_{\rm DE}, 2.12\Omega_{\rm DE})$, i.e., $(1.19, 1.57)$ after imposing $\Omega_{\rm DE} = 0.74$. On the other hand, we obtained a lower bound, but without an upper bound, to $|\omega|$ with regard to the extent of the soft violation of the detailed balance condition. The lower bound depends on Λ_W, and in most cases it is also around the order of the inverse square of the Hubble length, H_0^2/c^2.

With our more comprehensive investigation into the cosmic-expansion test of Hořava gravity, we found the Hořava effective dark energy (*HEDE*) much more restrictive than that deduced in [60]. Specifically, the allowed parameter space $\{w_0, w_a\}$ is now much smaller. It is a narrow strip beside the parabola $1+4w_0+3w_0^2+w_a = 0$ around $(w_0, w_a) = (-1, 0)$. The energy density of the *HEDE*, with different values of the model parameters, can give rise to a cosmological constant as well as non-constant behaviors. For the latter cases with non-constant energy density, the main difference between the models therein is the evolution of the dark energy density in the "middle age". This is because during the "middle age" the curvature-like (Ω_2) term dominates, while the range of allowed Ω_2 is not small, namely from -0.04 to $+1.03$. As a result the dark energy behavior in the non-constant cases almost coincide with each other at high redshifts. This is because in the early times the dark energy is dominated by the radiation-like (Ω_1) term that is highly restricted, namely $\Omega_1 \lesssim 8.47\times10^{-5}$.

In our analysis we compare *HEDE* with observational results by invoking the CPL parametrization of the equation of state of dark energy: $w_{\rm DE} = w_0+w_a(1-a)$, as a mediator. We then transfer the constraint on the phenomenological parameters $\{\Omega_k, \Omega_{\rm DE}, w_0, w_a\}$ to that on the model parameters $\{\Omega_k, \omega, \Lambda_W\}$ via an approximate relation between $\{w_0, w_a\}$ and $\{\Omega_k, \omega, \Lambda_W\}$. Naively, since the dimension of the phenomenological parameter space is larger than that of the model space, the 4D parameter space seems flexible enough to

accommodate the mapping from the 3D model space. Nevertheless, to be prudent, the validity of this approximation should be checked. In particular, it is important to verify that the two energy densities, $\rho_{\rm HEDE}(z;\Omega_k,\omega,\Lambda_W)$ and $\rho_{\rm CPL}(z;\Omega_{\rm DE},w_0,w_a)$, are consistent with each other, where $\rho_{\rm HEDE}$ is given in Eqs. (2.10) or (2.13) and

$$\rho_{\rm CPL}=\rho_0 e^{3w_a(a-1)}a^{-3(1+w_0+w_a)}. \tag{7.1}$$

The approximation is valid when the difference between these two energy densities is significantly smaller than the observational accuracy in the relevant redshift range. This consistency check requires further investigation. One way to avoid the possible incompatibility between the model space and the phenomenological parameter space is to use the model to fit data directly, e.g., invoking the χ^2 fitting to obtain the observational constraints on the model parameters $\{\Omega_k,\Lambda_W,\omega\}$. This is under our investigation and will be reported in our follow-up paper.

Hořava gravity, an interesting alternative gravity theory that breaks the Lorentz symmetry, should ideally be constrained by observations and experiments ranging from microscopic, solar, astronomical, to cosmological scales. From the cosmological point of view, a modified gravity theory changes not only the cosmic expansion history but also the structure formation. In the present paper we have shown how the IR-modified Hořava gravity can be tightly constrained by the observations about the cosmic expansion. In addition to the expansion history, we expect the observations about the cosmic structures, such as galaxy surveys and weak lensing observations, would also provide important constraints on Hořava gravity. This is worthy of further investigations.

Acknowledgments

We thank Debaprasad Maity for his useful suggestions and comments on the subject. C.-I Chiang wishes to thank Shu-Heng Shao, Wei-Ting Lin, Kung-Yi Su, Che-Min Shen and Yeng-Ta Huang for useful and encouraging discussions. Chen is supported by Taiwan National Science Council under Project No. NSC97-2112-M-002-026-MY3, by Taiwan's National Center for Theoretical Sciences (NCTS), and by US Department of Energy under Contract No. DE-AC03-76SF00515. Gu is supported by the Taiwan National Science Council under Project No. NSC 98-2112-M-002-007-MY3.

References

[1] P. Horava, *Quantum Gravity at a Lifshitz Point*, *Phys. Rev.* **D79** (2009) 084008, [arXiv:0901.3775].

[2] P. Horava, *Membranes at Quantum Criticality*, *JHEP* **03** (2009) 020, [arXiv:0812.4287].

[3] R.-G. Cai, Y. Liu, and Y.-W. Sun, *On the z=4 Horava-Lifshitz Gravity*, *JHEP* **06** (2009) 010, [arXiv:0904.4104].

[4] R.-G. Cai, B. Hu, and H.-B. Zhang, *Dynamical Scalar Degree of Freedom in Horava-Lifshitz Gravity*, *Phys. Rev.* **D80** (2009) 041501, [arXiv:0905.0255].

[5] T. Nishioka, *Horava-Lifshitz Holography*, *Class. Quant. Grav.* **26** (2009) 242001, [arXiv:0905.0473].

[6] C. Charmousis, G. Niz, A. Padilla, and P. M. Saffin, *Strong coupling in Horava gravity*, *JHEP* **08** (2009) 070, [arXiv:0905.2579].

[7] T. P. Sotiriou, M. Visser, and S. Weinfurtner, *Quantum gravity without Lorentz invariance*, *JHEP* **10** (2009) 033, [arXiv:0905.2798].

[8] C. Germani, A. Kehagias, and K. Sfetsos, *Relativistic Quantum Gravity at a Lifshitz Point*, *JHEP* **09** (2009) 060, [arXiv:0906.1201].

[9] A. Kobakhidze, *On the infrared limit of Horava's gravity with the global Hamiltonian constraint*, arXiv:0906.5401.

[10] C. Bogdanos and E. N. Saridakis, *Perturbative instabilities in Horava gravity*, *Class. Quant. Grav.* **27** (2010) 075005, [arXiv:0907.1636].

[11] J. Kluson, *Horava-Lifshitz f(R) Gravity*, *JHEP* **11** (2009) 078, [arXiv:0907.3566].

[12] N. Afshordi, *Cuscuton and low energy limit of Horava-Lifshitz gravity*, *Phys. Rev.* **D80** (2009) 081502, [arXiv:0907.5201].

[13] Y. S. Myung, *Generalized uncertainty principle and Hořava-Lifshitz gravity*, *Phys. Lett.* **B679** (2009) 491–498, [arXiv:0907.5256].

[14] J. Alexandre, K. Farakos, P. Pasipoularides, and A. Tsapalis, *Schwinger-Dyson approach for a Lifshitz-type Yukawa model*, *Phys. Rev.* **D81** (2010) 045002, [arXiv:0909.3719].

[15] D. Blas, O. Pujolas, and S. Sibiryakov, *A healthy extension of Horava gravity*, arXiv:0909.3525.

[16] D. Capasso and A. P. Polychronakos, *Particle Kinematics in Horava-Lifshitz Gravity*, *JHEP* **02** (2010) 068, [arXiv:0909.5405].

[17] B. Chen, S. Pi, and J.-Z. Tang, *Power spectra of scalar and tensor modes in modified Horava-Lifshitz gravity*, arXiv:0910.0338.

[18] J. Kluson, *New Models of f(R) Theories of Gravity*, *Phys. Rev.* **D81** (2010) 064028, [arXiv:0910.5852].

[19] E. Kiritsis, *Spherically symmetric solutions in modified Horava- Lifshitz gravity*, *Phys. Rev.* **D81** (2010) 044009, [arXiv:0911.3164].

[20] R. Garattini, *The cosmological constant as an eigenvalue of the Hamiltonian constraint in Horava-Lifshits theory*, arXiv:0912.0136.

[21] J. Kluson, *String in Horava-Lifshitz Gravity*, arXiv:1002.2849.

[22] E. J. Son and W. Kim, *Smooth cosmological phase transition in the Horava- Lifshitz gravity*, arXiv:1003.3055.

[23] S. Carloni *et al.*, *Modified first-order Horava-Lifshitz gravity: Hamiltonian analysis of the general theory and accelerating FRW cosmology in power-law F(R) model*, arXiv:1003.3925.

[24] M. Eune and W. Kim, *Note on an action for a particle in the Hořava- Lifshitz Gravity*, arXiv:1003.4052.

[25] M. Li and Y. Pang, *A Trouble with Hořava-Lifshitz Gravity*, *JHEP* **08** (2009) 015, [arXiv:0905.2751].

[26] M. Visser, *Lorentz symmetry breaking as a quantum field theory regulator*, *Phys. Rev.* **D80** (2009) 025011, [arXiv:0902.0590].

[27] D. Blas, O. Pujolas, and S. Sibiryakov, *On the Extra Mode and Inconsistency of Horava Gravity*, *JHEP* **10** (2009) 029, [arXiv:0906.3046].

[28] M. Henneaux, A. Kleinschmidt, and G. L. Gomez, *A dynamical inconsistency of Horava gravity*, *Phys. Rev.* **D81** (2010) 064002, [arXiv:0912.0399].

[29] J. M. Pons and P. Talavera, *Remarks on the consistency of minimal deviations from General Relativity*, arXiv:1003.3811.

[30] J. Bellorin and A. Restuccia, *On the consistency of the Horava Theory*, arXiv:1004.0055.

[31] G. Calcagni, *Cosmology of the Lifshitz universe*, *JHEP* **09** (2009) 112, [arXiv:0904.0829].

[32] E. Kiritsis and G. Kofinas, *Horava-Lifshitz Cosmology*, *Nucl. Phys.* **B821** (2009) 467–480, [arXiv:0904.1334].

[33] M. Chaichian, S. Nojiri, S. D. Odintsov, M. Oksanen and A. Tureanu, *Modified F(R) Horava-Lifshitz gravity: a way to accelerating FRW cosmology*, arXiv:1001.4102.

[34] E. Elizalde, S. Nojiri, S. D. Odintsov and D. Saez-Gomez, *Unifying inflation with dark energy in modified F(R) Horava-Lifshitz gravity*, arXiv:1006.3387.

[35] X. Gao, Y. Wang, R. Brandenberger, and A. Riotto, *Cosmological Perturbations in Hořava-Lifshitz Gravity*, *Phys. Rev.* **D81** (2010) 083508, [arXiv:0905.3821].

[36] S. Mukohyama, *Scale-invariant cosmological perturbations from Horava- Lifshitz gravity without inflation*, *JCAP* **0906** (2009) 001, [arXiv:0904.2190].

[37] Y.-S. Piao, *Primordial Perturbation in Horava-Lifshitz Cosmology*, *Phys. Lett.* **B681** (2009) 1–4, [arXiv:0904.4117].

[38] B. Chen, S. Pi, and J.-Z. Tang, *Scale Invariant Power Spectrum in Hořava-Lifshitz Cosmology without Matter*, *JCAP* **0908** (2009) 007, [arXiv:0905.2300].

[39] Y.-F. Cai and X. Zhang, *Primordial perturbation with a modified dispersion relation*, *Phys. Rev.* **D80** (2009) 043520, [arXiv:0906.3341].

[40] A. Wang and R. Maartens, *Linear perturbations of cosmological models in the Horava-Lifshitz theory of gravity without detailed balance*, *Phys. Rev.* **D81** (2010) 024009, [arXiv:0907.1748].

[41] T. Kobayashi, Y. Urakawa, and M. Yamaguchi, *Large scale evolution of the curvature perturbation in Horava-Lifshitz cosmology*, *JCAP* **0911** (2009) 015, [arXiv:0908.1005].

[42] X. Gao, *Cosmological Perturbations and Non-Gaussianities in Hořava-Lifshitz Gravity*, arXiv:0904.4187.

[43] T. Kobayashi, Y. Urakawa, and M. Yamaguchi, *Cosmological perturbations in a healthy extension of Horava gravity*, *JCAP* **1004** (2010) 025, [arXiv:1002.3101].

[44] E. Kiritsis and G. Kofinas, *On Horava-Lifshitz 'Black Holes'*, *JHEP* **01** (2010) 122, [arXiv:0910.5487].

[45] M.-i. Park, *The Black Hole and Cosmological Solutions in IR modified Horava Gravity*, *JHEP* **09** (2009) 123, [arXiv:0905.4480].

[46] U. H. Danielsson and L. Thorlacius, *Black holes in asymptotically Lifshitz spacetime*, *JHEP* **03** (2009) 070, [arXiv:0812.5088].

[47] R.-G. Cai, L.-M. Cao, and N. Ohta, *Topological Black Holes in Horava-Lifshitz Gravity*, *Phys. Rev.* **D80** (2009) 024003, [arXiv:0904.3670].

[48] A. Kehagias and K. Sfetsos, *The black hole and FRW geometries of non-relativistic gravity*, *Phys. Lett.* **B678** (2009) 123–126, [arXiv:0905.0477].

[49] Y. S. Myung, *Thermodynamics of black holes in the deformed Hořava- Lifshitz gravity*, *Phys. Lett.* **B678** (2009) 127–130, [arXiv:0905.0957].

[50] M. Botta-Cantcheff, N. Grandi, and M. Sturla, *Wormhole solutions to Horava gravity*, arXiv:0906.0582.

[51] H. W. Lee, Y.-W. Kim, and Y. S. Myung, *Extremal black holes in the Hořava-Lifshitz gravity*, arXiv:0907.3568.

[52] J. Greenwald, A. Papazoglou, and A. Wang, *Black holes and stars in Horava-Lifshitz theory with projectability condition*, *Phys. Rev.* **D81** (2010) 084046, [arXiv:0912.0011].

[53] B. R. Majhi, *Hawking radiation and black hole spectroscopy in Horava- Lifshitz gravity*, *Phys. Lett.* **B686** (2010) 49–54, [arXiv:0911.3239].

[54] G. Koutsoumbas, E. Papantonopoulos, P. Pasipoularides, and M. Tsoukalas, *Black Hole Solutions in 5D Horava-Lifshitz Gravity*, *Phys. Rev.* **D81** (2010) 124014, [arXiv:1004.2289].

[55] T. Takahashi and J. Soda, *Chiral Primordial Gravitational Waves from a Lifshitz Point*, *Phys. Rev. Lett.* **102** (2009) 231301, [arXiv:0904.0554].

[56] S. Mukohyama, K. Nakayama, F. Takahashi, and S. Yokoyama, *Phenomenological Aspects of Horava-Lifshitz Cosmology*, *Phys. Lett.* **B679** (2009) 6–9, [arXiv:0905.0055].

[57] Y. S. Myung, *Chiral gravitational waves from z=2 Hořava-Lifshitz gravity*, *Phys. Lett.* **B684** (2010) 1–5, [arXiv:0911.0724].

[58] S. Koh, *Relic gravitational wave spectrum, the trans-Planckian physics and Hořava-Lifshitz gravity*, arXiv:0907.0850.

[59] M.-i. Park, *Horava Gravity and Gravitons at a Conformal Point*, arXiv:0910.5117.

[60] M.-i. Park, *A Test of Horava Gravity: The Dark Energy*, *JCAP* **1001** (2010) 001, [arXiv:0906.4275].

[61] E. N. Saridakis, *Horava-Lifshitz Dark Energy*, *Eur. Phys. J.* **C67** (2010) 229, [arXiv:0905.3532].

[62] M. Jamil and E. N. Saridakis, *New agegraphic dark energy in Horava-Lifshitz cosmology*, arXiv:1003.5637.

[63] A. Ali, S. Dutta, E. N. Saridakis, and A. A. Sen, *Horava-Lifshitz cosmology with generalized Chaplygin gas*, arXiv:1004.2474.

[64] S. Dutta and E. N. Saridakis, *Observational constraints on Horava-Lifshitz cosmology*, *JCAP* **1001** (2010) 013, [arXiv:0911.1435].

[65] S. Dutta and E. N. Saridakis, *Overall observational constraints on the running parameter lambda of Horava-Lifshitz gravity*, arXiv:1002.3373.

[66] H. Lu, J. Mei, and C. N. Pope, *Solutions to Horava Gravity*, *Phys. Rev. Lett.* **103** (2009) 091301, [arXiv:0904.1595].

[67] H. Nastase, *On IR solutions in Horava gravity theories*, arXiv:0904.3604.

[68] A. Kehagias and K. Sfetsos, *The black hole and FRW geometries of non-relativistic gravity*, *Phys. Lett.* **B678** (2009) 123–126, [arXiv:0905.0477].

[69] T. Kim and C. O. Lee, *Exact Solutions in IR modified Horava-Lifshitz Gravity*, arXiv:1002.0784.

[70] M. Chevallier and D. Polarski, *Accelerating universes with scaling dark matter*, *Int. J. Mod. Phys.* **D10** (2001) 213–224, [gr-qc/0009008].

[71] E. V. Linder, *Exploring the expansion history of the universe*, *Phys. Rev. Lett.* **90** (2003) 091301, [astro-ph/0208512].

[72] K. Ichikawa and T. Takahashi, *The Hubble Constant and Dark Energy from Cosmological Distance Measures*, *JCAP* **0804** (2008) 027, [arXiv:0710.3995].

[73] J.-Q. Xia, H. Li, G.-B. Zhao, and X. Zhang, *Determining Cosmological Parameters with Latest Observational Data*, *Phys. Rev.* **D78** (2008) 083524, [arXiv:0807.3878].

[74] C.-W. Chen, P. Chen, and J.-A. Gu, *Constraints on the Phase Plane of the Dark Energy Equation of State*, *Phys. Lett.* **B682** (2009) 267–273, [arXiv:0905.2738].

[75] E. Komatsu *et al.*, *Seven-Year Wilkinson Microwave Anisotropy Probe (WMAP) Observations: Cosmological Interpretation*, arXiv:1001.4538.

[76] D. Larson *et al.*, *Seven-Year Wilkinson Microwave Anisotropy Probe (WMAP) Observations: Power Spectra and WMAP-Derived Parameters*, arXiv:1001.4635.

[77] M.-i. Park, *Holography in Three-dimensional Kerr-de Sitter Space with a Gravitational Chern-Simons Term*, *Class. Quant. Grav.* **25** (2008) 135003, [arXiv:0705.4381].

[78] G. Calcagni, *Detailed balance in Horava-Lifshitz gravity*, *Phys. Rev.* **D81** (2010) 044006, [arXiv:0905.3740].